QIRT 10
http://dx.doi.org/10.21611/qirt.2010.012
10th International Conference on Quantitative InfraRed Thermography
July 27-30, 2010, Québec (Canada)

Large dimension photothermal screen for the characterization of very short pulsed microwave fields using infrared thermography

by Daniel L. Balageas, Patrick Levesque

ONERA, Dept. of Composite Materials and Structures, BP 72, 92322 Châtillon, France
daniel.balageas@onera.fr

Abstract

The characterization on the field of large dimensions, high-energy, ultra short pulsed microwave fields by the combined use of an infrared camera and a photothermal film bonded on low density dielectric baking layer, due to the complexity of the pulse thermal response of such transducers, requires a modelling and an identification strategy. A model has been developed and numerical simulations permitted the definition of a fluence identification strategy adapted to the thermographic information processing. An experimental validation has been carried out at the CEA Research Center of Gramat using an electromagnetic source delivering pulses of 15 ns duration.

1. Introduction

Illumination of a sample by a photonic beam and mapping of its surface temperature using infrared thermography is a commonly used procedure for a wide spectrum of applications: i) identification of thermal properties, ii) detection and characterization of possible embedded defects causing local disturbances of the temperature field (non-destructive applications), iii) identification of the heat transfer existing between the sample the surroundings - fluid flows in particular -, iv) identification of the incident flux of energy.

In the last case, the sample is not the subject of the measurement. It plays the role of a sensor, or to be more precise, it is a photothermal converter. This type of application is mainly used in the domain of microwaves and is the subject of a specialized literature (Balageas et al., 1993; Norgard and Musselman, 2005a,b; Levesque et al., 2005). The present work describes an application of this type, limited to short pulse electromagnetic fields (Dirac). In this case, the parameter to be identified is not the intensity (incident power density), but the fluence (incident energy density).

The development and validation of a microwave sensitive screen adapted to the characterization on the field of large dimensions, high-energy, ultra short pulsed microwave fields are presented.

All the photohermal converters considered are films, which can be essentially divided in two types: air backed films and foam-backed films. These film-converters can be also ranked in two classes: surface- and volume-absorbing films. By the way, we will consider in sections 2 and 3 four different configurations: surface- and volume absorbing, air- and foam-backed films. Considering the specific case of the screen developed at ONERA (section 4), the direct problem will be solved to understand the thermal behavior of the converters during the measurements (sections 5 and 6). In section 7, experimental validation of the numerical approach will be presented, which will allow to define in section 8 the best procedure for the fluence identification

2. The different types of film-converters

2.1. Surface- and volume-absorbing films

There are essentially two types of photothermal films :

- Films in which the photon-heat conversion takes place at the surface (film opaque for the incident radiations). For microwave beams, such film-converters can be a dielectric films with an electrically conducting sub-micronic coating (Levesque et al., 2005).
- Films which absorb the incident radiations in their volume (semi-transparent films). For microwave beams this type of converter can be made of a carbon loaded dielectric material - generally, Kapton is used – (Norgard and Musselman, 2005a) or ferrite loaded epoxies (Norgard et al., 1993). In the first case, the film is sensitive to the electric field, in the second one to the magnetic field. For films moderately absorbing, the absorption can be considered as uniform in the depth of the film. This assumption will be made here.

2.2. Air-backed and foam-backed films

For practical applications, the film can be fixed on a rigid frame. In this case, the film in its central area used for the measurement, can be considered as self-standing film. This is an “air-backed” film (ABF). On both sides of the film, radiative and convective heat losses take place. If the film temperature increase due to the photothermal conversion is moderate (a few Kelvin), the heat losses can be considered as linearly proportional to the temperature increase of the film and characterized by a mixed heat transfer coefficient, h.

http://dx.doi.org/10.21611/qirt.2010.012
10th International Conference on Quantitative InfraRed Thermography

When the dimensions of the electromagnetic field to characterize are large, the stiffness of this converter is questionable, especially when the measurement take place outdoors (windy conditions, temperature and humidity variations…). A solution commonly used (Norgard and Musselman, 2005a) consists in bonding the film to a slab of low density dielectric foam (backing substrate). This type of film is a foam-backed film (FBF). The absorption in the foam will be considered as negligible and the heat losses of the film by radiation and convection are divided by a factor of two, since they take place just on the front-face of the film. Nevertheless, in this case, there are drawbacks:

- heat losses by conduction from the film to the foam exist, which are not easily estimated,
- uniformity of the bonding (thickness regularity in particular) can be questionable. If the bonding is locally imperfect, a thermal resistance at the interface introduces a perturbation in the temperature field of the system, which may change the sensitivity coefficient of the photothermal converter (the coefficient relating the temperature increase to the local fluence of the incident electric field pulse).

In a first step (section 5) the bonding layer will supposed negligible compared to the photothermal film. In a second step a three-layer slab model will be used (section 6).

3. Modeling of the various types of photothermal screens

The four types of photothermal screens introduced in the preceding section are presented in Figure 1. For each type of screen, analytical or semi-analytical solutions exist describing the pulse thermal response (surface temperature increase ΔT as a function of time, t, with $t = 0$ at the pulse occurrence).

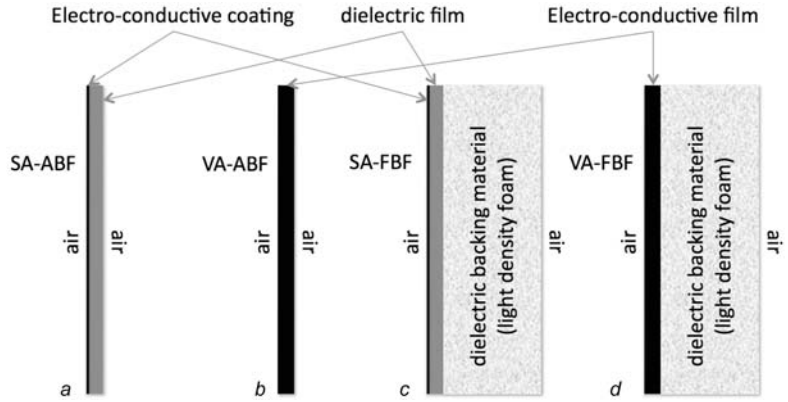

Figure 1. *The various types of photothermal screens for imaging micro-wave fields: a) Surface-Absorption Air-backed Film (SA-ABF), b) Volume-Absorption Air-Backed Film (VA-ABF), c) Surface-Absorption Foam-backed Film (SA-FBF), b) Volume-Absorption Foam-Backed Film (VA-ABF),*

- Volume-absorption air-backed film (VA-ABF): for adiabatic conditions, the film behaves like a calorimeter. The temperature increase is constant and equal to the adiabatic temperature increase, ΔT_{adia}:

$$\Delta T = \Delta T_{adia} = Q/(\rho CL)_f . \qquad (1)$$

with Q the absorbed fluence, and L_f and $(\rho C)_f$ respectively the thickness and the volume heat capacity of the film. For heat losses at the front and rear faces the expression is the following:

$$\Delta T / \Delta T_{adia} = \exp[-2ht/(\rho CL)_f] \qquad (2)$$

- Surface-absorption air-backed film (SA-ABF): for adiabatic conditions, the film follows the law

$$\Delta T / \Delta T_{adia} = 1 + 2\sum_1^\infty \exp(-n^2\pi^2\kappa_f t / L_f^2) = 1 + 2\sum_1^\infty \exp(-n^2\pi^2 Fo_f), \qquad (3)$$

κ and Fo being respectively the thermal diffusivity and the Fourier number of the film.

For heat losses at the limits an analytical solution exists:

$$\Delta T / \Delta T_{adia} = (1/Bi)\sum_1^\infty \mu_n^2 \exp(-\mu_n^2 Fo_f)(2\sin\mu_n.\cos\mu_n)/(\mu_n + \sin\mu_n.\cos\mu_n) \qquad (4)$$

$Bi = h.L/k$ being the Biot number and μ_n the positive roots of: $\mu.tg\mu = Bi$.

- The FBFs need the use of two-layer models and can be solved by a semi-analytical approach which consists to use the Laplace transform and the thermal quadrupole method [6] followed by a return to the real space using the Stehfest algorithm [7]. For surface absorption (SA-FBF) with adiabatic conditions and resistive interface, an analytical solution can be find in Ref. [8], and for a thermally semi-infinite backing layer with perfect interface a simple analytical solution is proposed by Ref. [9]:

http://dx.doi.org/10.21611/qirt.2010.012

$$\Delta T = (Q / e_f \sqrt{\pi} \sqrt{t}\,)\,[1 + 2\sum_1^{\infty} (-\Gamma)^n \exp(-n^2 L_f^2 / \kappa_f t)] = (Q / e_f \sqrt{\pi} \sqrt{t}\,)\,[1 + 2\sum_1^{\infty} (-\Gamma)^n \exp(-n^2 / Fo_f)] \qquad (5)$$

with e_f the film effusivity and Γ the thermal mismatch factor (or reflection coefficient): $\Gamma=(e_b-e_f)/e_b+e_f)$, e_b being the backing effusivity.

4. Technological solution adopted for the screen

The practical fabrication of a foam-backed film requires bonding of the film on the backing material. ONERA has optimized a foam-backed film configuration constituted by:

- a photothermal film made of a Carbon-loaded Teflon™ (polyimide) manufactured by Dupont de Nemours & Co., with a mean thickness of 38.1 ± 0.8 µm. Regarding the electric properties, two grades of square resistance exist: 375 and 1200 Ω/□. This film has a volume absorption. The total absorption of the film being moderate (for instance 24% for the 1200 Ω/□ film) the absorption can be considered, as a first approximation, as uniform through the film depth.
- a foam made of extruded polystyrene (Jackodur ZL 35-300, produced by Geniflex-Jackson S.A., Belgium) of density 34 kg m^{-3} and thickness 40 mm.
- a bond made of 3M™ Fastbond™ 30.

Such a system permits the elaboration of photothermal panels of several m^2. The screen is of the VA-FBF type.

The existence of a bonding layer may cause discrepancies between reality and the two-layer model used if this layer has a thickness of the same order of magnitude as the one of the film. Microscopic analysis of the bonding region shows that the layer thickness is variable, due to the foam roughness, with a mean value near of 20 µm (see Figure 2). At a macroscopic scale (the scale of a pixel of the thermal image, i.e. several millimeters for a panel of several square meters) the bond layer thickness can be considered as uniform. The equivalent thermal resistance is, considering the nature of the bond: $R_{bond} = (L/k)_{bond}$ = 0.00008 $W^{-1}m^2K$, a low value which corresponds to a good thermal contact. Nevertheless, the existence of the bond layer has a second effect on the heat diffusion due to its heat capacity $(\rho CL)_{bond}$. In the present case, $(\rho CL)_{bond} / (\rho CL)_{film}$ = 0.5, which requires to take into account the existence of the bond layer in the model, using a more sophisticated approach. This is accomplished by the use of a 3-layer model. The values of the thermophysiqcal parameters used with the 2- and 3-layer models are presented in Table 1.

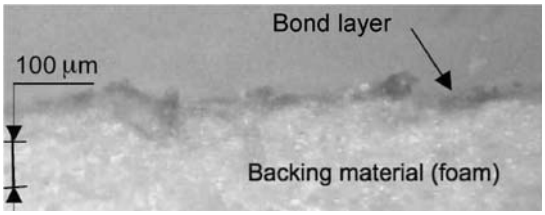

Figure 2. *Microscope image of the bond layer (3M™Fastbond™ 30) on the backing material (light density foam) showing a mean thickness of 20 µm.*

Table 1. *Values given to the thermophysical parameters used for the theoretical evaluations (2-layer model of section 5 and 3-layer model of section 6).*

	Two-layer model and generic thermophysical parameters used for the comparison of the various types of microwave sensitive photothermal screens					Three-layer model and thermophysical parameters representative of the screen developed at ONERA used for the evaluations presented in section 6						
Parameters	Environ-ment	Photo-thermal film	Interface	Backing material	Environ-ment	Environ-ment	Photo-thermal film	Interface	Bond layer	Interface	Backing material	Environ-ment
Heat transfer coeff., h ($Wm^{-2}K^{-1}$)	0 - 10				0 - 10	0 - 10						0 - 10
Thickness, L (µm)		50		1,500			38		0 - 19 - 38		1,500	
Thermal conductivity, k ($Wm^{-1}K^{-1}$)		0.25		0.05			0.12		0.25		0.035	
Volume heat capacity, ρC (MJ $m^{-3}K^{-1}$)		1.2		0.12			1.54		1.2		0.048	
Thermal resistance, R ($W^{-1}m^2K$)			0 - 0.001					0 - 0.005		0 - 0.005		

5. Thermal behavior of the various types of screens

The pulsed thermograms of the four types of screens are presented in a log-log plot in the Figure 3. The general trends are the following:

- For very short times following the pulse (< 2ms for the properties of the developed screen), the thermal response is essentially influenced by the type of absorption and absolutely not by the possible existence of a backing. For

http://dx.doi.org/10.21611/qirt.2010.012
10th International Conference on Quantitative InfraRed Thermography

surface absorption the thermogram is that of the semi-infinite medium, a straight line in log-log with slope -0.5 (ΔT proportional to $1/\sqrt{t}$). The identification of the absorbed fluence needs to know the effusivity of the film. For volume absorption screens, the temperature is the adiabatic plateau equal to $Q/(\rho CL)_f$ from which the absorbed fluence is instantaneously deduced

$$Q = (\rho CL)_f \, \Delta T_{adia} \qquad (6)$$

- For larger times, the thermogram are no more influenced by the type of absorption, but depends on the structural arrangement of the screen (backing or not, thermally perfect or imperfect interface). For both VA-ABF and SA-ABF the adiabatic temperature increase remains for times up to 30 ms, a period during which the formula (6) can be used for identifying the absorbed fluence. For t > 30 ms the thermograms are more and more influenced by heat losses, which impede the absorbed fluence identification in good conditions. For both VA-FBF and SA-FBF and for times t >2 ms the shape of the thermogram is more complicated and depends on the structural arrangement (thicknesses) and thermal properties of the screen components (diffusivity and effusivity, interface thermal resistances) and on the heat losses at boundaries, making the identification difficult and not precise.
- Finally, it appears that the addition of a foam baking complicates the identification and strongly reduces the period during which a precise and simple identification of the absorbed fluence is possible (from 30 ms to 2 ms).

All these numbers are just given for information, since they are based on approximate values of the thermal parameters and on a simplified 2-layer model. Nevertheless, the orders of magnitude are pertinent and must be regarded as guides for the elaboration of an identification strategy. They will be refined in followings sections thanks to the use of 3-layer model.

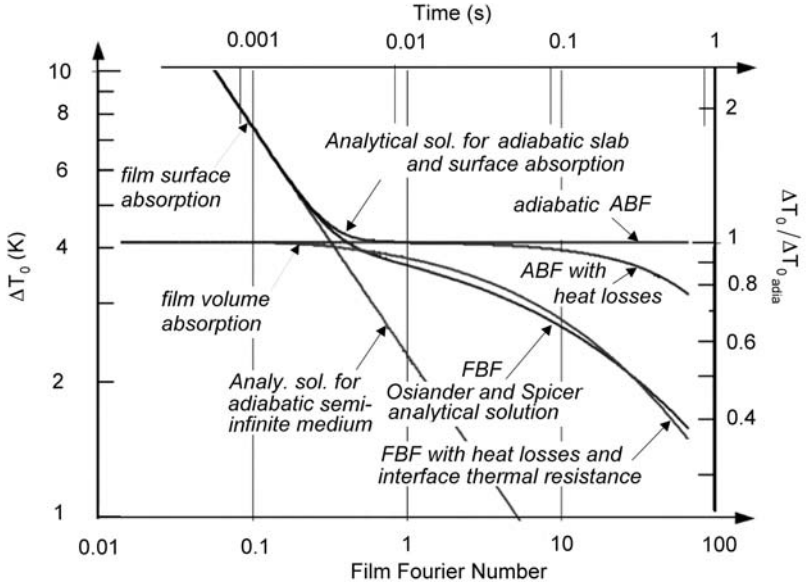

Figure 3. *Comparison between air-backed (one-layer model) and foam-backed (two-layer model) films, with surface or volume absorption, adiabatic conditions or heat losses (h = 10 W $m^{-2}K^{-1}$) at the limits, perfect or imperfect (R = 0.001 $W^{-1}m^2K$) interface.*

6. Theoretical evaluation of the pulse response of the screen developed at ONERA

The screen developed is of the type VA-FBF (volume-absorption foam-backed film). As seen in the conclusions of section 5, for VA-FBF screen the best strategy for a satisfactory identification of the fluence consists to operate at the very beginning of the cooling phase just after the pulse. The initial adiabatic plateau last a few milliseconds, which is the delicate point of the measurement with an infrared camera. Thus the aim of the present theoretical study is double: i) to get a good estimate of the duration of the plateau, ii) to study the influence of the variability of the bond layer on the scatter of thermal response from point to point in such a large screen. A third point has to be explored: supposing that no synchronization between the pulse source and the infrared camera exists, evaluate the combined influence of the frame rate and of the method used to estimate the initial temperature increase on the the final result. This study will be carry out using experimental data and presented in section 7.

The presence of the bond requires to use a 3-layer model. We chose to solve the system using the Euler finite difference method in 1-D. This very simple method is so simple that it has been written under the form of an Excel spread-sheet. Its only drawback is that the calculation can easily become instable, which requires to be very careful in the choice of time and space steps and involves a high number of time step. Typical calculations have been done with 50 nodes and up to 32,000 time steps. The thermophysical properties given to the various components of the screen are detailed in Table 1. Regarding the bond layer, we supposed that its thickness could varies between 0 and twice its mean observed value, 38 μm, which is the thickness of the film.

http://dx.doi.org/10.21611/qirt.2010.012

6.1. Estimation of the initial adiabatic plateau and influence of the various components of the screen on its duration.

Figure 4 presents the thermograms for the three bond thicknesses of 0, 19, and 38 μm. The heat losses are supposed corresponding to a heat transfer coefficient h = 10 W $m^{-2}K^{-1}$ and the thermal resistance of the interfaces (film/bond and bond/backing) is taken equal to 0.0005 W^{-1} m^2 K. The corresponding VA-ABF result is also given for comparison.

The first impression is that the shape of the thermograms is notably different from the one seen with the 2-layer model. This is due the bond. Nevertheless, the result for a zero bond thickness is coherent with the result of the 2-layer model. The shapes in this case are identical and the adiabatic plateau duration, evaluated in Fourier number are the same: near 0.2. The plateau durations, evaluated in physical time, are different, which is due to the fact that the thermal properties and thickness of the film assumed for the preliminary calculation with the 2-layer model are different from the ones adopted for the screen effectively developed.

The bond thickness as a strong influence on the shape of the thermogram for time higher than10 ms. The duration of the adiabatic plateau is influenced, passing from 5 ms to 2 ms when the thickness increases from 0 to 19 μm. For a higher thickness no decrease of the plateau duration appears. In comparison, the plateau of the air-backed film is one order of magnitude longer (roughly 50 ms).

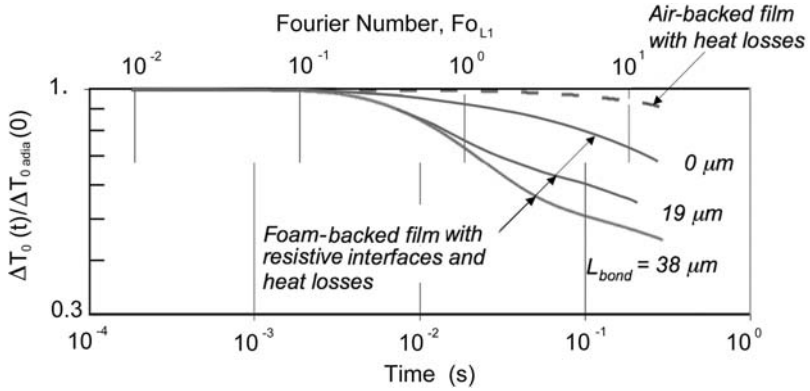

Figure 4. *Influence of the bond thickness on the pulse thermograms for the screen developed at ONERA. Heat losses and interface thermal resistances are respectively taken equal to 0.0005 $W^{-1}m^2K$ and 10 $Wm^{-2}K^{-1}$.*

6.2 Scatter due to the variability of the bond layer in a large screen

The identification of the fluence by estimating the initial adiabatic temperature increase requires to know the pulse time, and to extrapolate the thermogram to this time. The very short duration of the initial plateau makes the influence of the uncertainty on this time of prime importance. A solution consists in supposing that the pulse occurs at half an acquisition period before the time of the first image following the pulse (the first image showing an increase of temperature). In this case, the uncertainty on the pulse occurrence is limited to this half period. Two simple methods can be used for identifying the adiabatic initial temperature:

- likening the temperature increases of the first image following the pulse to the initial adiabatic temperature increases, $\Delta T_{adia} = \Delta T^1 = T^1 - T^0$, T^1 and T^0 being respectively the temperatures in the images following and preceding the pulse,
- extrapolating linearly, from the first two images following the pulse, to the occurrence time supposed to be at an half acquisition period before the first image: $\Delta T_{adia} = 1.5\,\Delta T^1 - 0.5\,\Delta T^2$.

The two methods must lead to similar results when the acquisition frequency is high. We will choose the second method to evaluate the influence of the variability of the bond layer in a large screen on the identified fluence. Several local bonding conditions have been considered (Figure 5): absence of bond, nominal bond thickness (19 μm) and over-thickness (38 μm), combined with perfect contact between film and bond (null thermal resistance), imperfect contact (R = 0.001 $W^{-1}m^2K$) which is equivalent to 25 μm of air and could be caused by irregularities and roughness of the foam, and existence of air blisters (macroscopic inclusions of air between film and bond layer) corresponding to an infinite value of the thermal contact resistance. Thus, nine different types of local conditions have been defined and modelled using 1-layer, 2-layer and 3-layer models. For each case, the theoretical thermogram has been digitized with three acquisition frequencies: 125, 250 and 500 Hz.

Table 2 presents the resulting accuracy for all these conditions. The accuracy is strongly dependent on both these local conditions and the frame rate. Paradoxically, the better accuracy is obtained in defective bond regions, in particular when blisters exists (in this case the film can be considered as an air-backed film).

The main conclusion from this simulation is the need to use high frame rates to guarantee a good uniformity and accuracy. So, to get accuracies better than 2% it is necessary to use a minimum frame rate of 500 Hz. It must be emphasized that these accuracies are essentially due to the uncertainty on the real occurrence time of the pulse. If a perfect synchronisation between the source and the camera is achieved lower image rates are acceptable. Furthermore, no intrinsic noise of the thermographic signal is assumed. Thus, the accuracies of Table 5 must be considered as minimum estimates and must be refined by data processing of real data (see section 7).

http://dx.doi.org/10.21611/qirt.2010.012
10th International Conference on Quantitative InfraRed Thermography

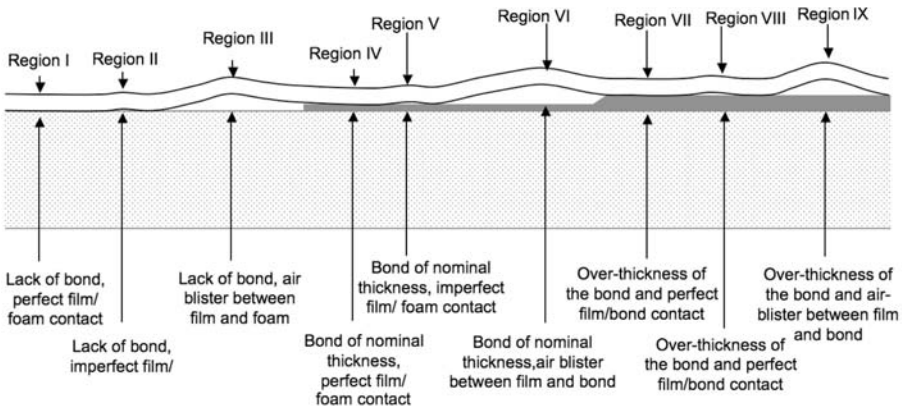

Figure 5. *Possible variability of the bond layer in a foam backed film of large dimension like the one developed at ONERA.*

Table 2. *Accuracy of the fluence identified by linear extrapolation from the first two images following the pulse for the ONERA photo-thermal screen. Influence of the frame rate of the infrared camera and of the local bonding conditions.*

Bond thickness (microns)	Interface resistance R ($W^{-1}m^2K$)	Heat transfer coefficient ($Wm^{-2}K^{-1}$)	Acquisition rate (Hz) / Error bounds (%)	125	250	500	Type of model used for simulation	Physical configuration of the photothermal converter system
0	0	0	Maximum	2.4%	1.1%	0.3%	2-layer model	Region I
			Minimum	-3.3%	-0.9%	0.2%		
	0.001	10	Maximum	1.8%	0.7%	0.2%	2-layer model	Region II
			Minimum	-2.0%	-0.3%	0.2%		
	infinite	10	Maximum	0.2%	0.1%	0.1%	1-layer model	Region III
			Minimum	-0.2%	-0.2%	-0.1%		
19	0	0	Maximum	10%	4.8%	1.2%	3-layer model	Region IV
			Minimum	-17%	-3.7%	1.2%		
	0.001	10	Maximum	5.5%	1.9%	0.8%	3-layer model	Region V
			Minimum	-6.0%	-0.1%	0.4%		
	infinite	10	Maximum	0.2%	0.1%	0.1%	1-layer model	Region VI
			Minimum	-0.2%	-0.2%	-0.1%		
38	0	0	Maximum	12%	5.0%	1.8%	3-layer model	Region VII
			Minimum	-17%	-2.7%	-1.1%		
	0.001	10	Maximum	5.8%	1.9%	0.8%	3-layer model	Region VIII
			Minimum	-5.4%	0.1%	0.4%		
	infinite	10	Maximum	0.2%	0.1%	0.1%	1-layer model	Region IX
			Minimum	-0.2%	-0.2%	-0.1%		
				-17% to 12%	-3.7% to 4.8%	-0.1% to 1.8%		

7. Experimental results

The screen developed at ONERA was tested at the CEA Research Center of Gramat in both configurations: with and without a foam backing layer. The camera was a LW CEDIP Jade camera. The frequency rate was 1 kHz, thanks to a ¼ windowing (60 x 80 pixels). The pulsed illumination duration was 15 ns. The signal-to-noise ratio is low as seen in Figure 6 presenting a thermographic image taken 10 ms after the pulse, recorded with the 375 Ω/□ film without backing, the temperature increase at the center of the beam and the horizontal profile.

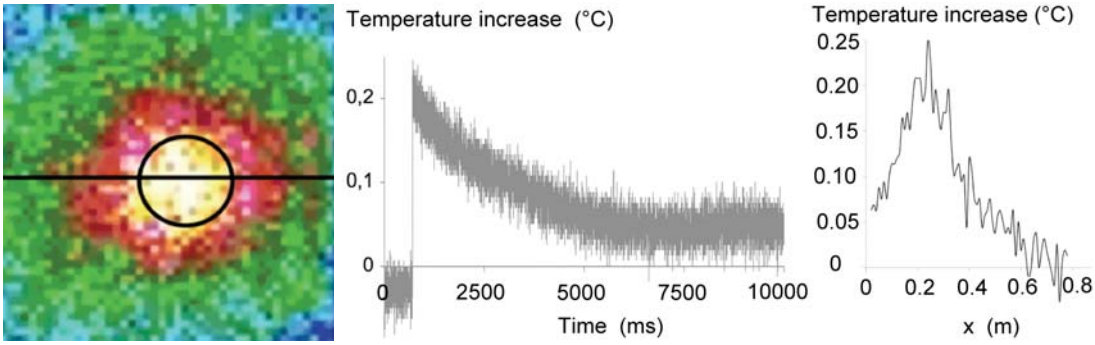

Figure 6. *Temperature increase of the ONERA 375 Ω/□ film without foam backing: (Left) Thermographic image of the center of the beam 10 ms after the pulse and circular area on which the mean temperature increase is calculated, (center) time evolution of the pixel at the center of the beam, (right) distribution on the horizontal line passing by the center of the beam.*

http://dx.doi.org/10.21611/qirt.2010.012

To improve the signal-to-noise ratio, the mean temperature increase of the circular area defined in Figure 6-left has been calculated by the ALTAIR software. This area contains near 700 pixels, which lead to a theoretical improvement of the signal-to-noise ratio of $\sqrt{700} \cong 26$. The mean thermograms obtained for both the air-backed and the foam-backed films are presented in Figure 7. The temperature increases $\Delta T(t)$ are normalized by those of the first image recorded after the pulse (ΔT^1). The noise is strongly reduced letting appear an unexplained very narrow-band noise at the frequency of 34.2 Hz, whose origin could be in the camera or in the electromagnetic environment. This noise is not detected when looking at the thermogram of a single pixel. Nevertheless, the thermograms of Figure 7 are easily interpretable. They show that the duration of the initial adiabatic plateau lasts roughly a few tens of milliseconds for the air-backed film and is reduced to less than 2 ms for the foam-backed film. This is in good agreement with the results of the numerical simulations shown in Figure 4.

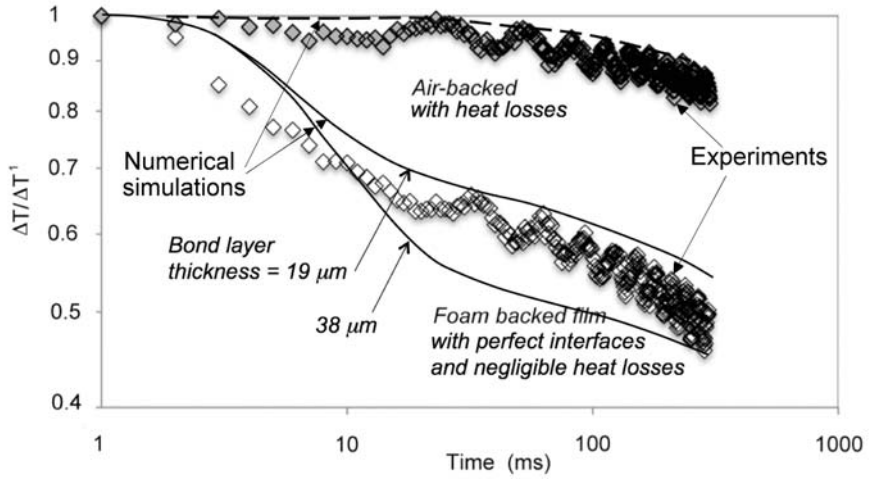

Figure 7. *Mean normalized temperature evolution in the center of the image (circular zone defined in Figure 6-left) monitored by the ONERA 375 Ω/□ film with and without a foam backing. Comparison of the first 300 ms showing the difference in the initial adiabatic plateau duration.*

Using the Euler finite difference model, a parametric study has been carry out to meet the experimental results of figure 7. Regarding the air-backed film, the thermal parameters of Table I for the film properties and heat losses on both faces with a heat transfer coefficient h = 10 W $m^{-2}K^{-1}$ have been assumed and lead to a simulated thermogram near of the experiment. The experimental thermogram of the foam-backed film is found near of the thermograms of a simulated screen with a bond layer between 19 and 38 μm, with perfect thermal contact at the interfaces and negligible heat losses. Nevertheless, a non-zero value of this coefficient h would have improve the agreement between experiment and simulation for times greater than 100 ms. Globally, we can conclude that the agreement is satisfying and that the model and the thermophysical parameters adopted for the simulations are relevant.

8. Choice of a strategy for the identification of the initial adiabatic plateau

The experiment being conducted with a frame rate of 1 kHz, it is possible to generate simulated experiments at lower frequencies. Thus, taking one image over two (for instance the even images) a 500 Hz thermographic record can be created. A second record at the same frequency is possible choosing the odd images. So, a 1 kHz experimental series generates two 500 Hz series. Similarly, it is possible to generate four 250 Hz series and eight 125 Hz series. For each frequency, each series has the same probability, and for each series it is possible to evaluate the pulse occurrence time (a need if no synchronization between the electromagnetic source and the camera exists) and develop the identification process using different approaches to estimate the initial adiabatic plateau value (and finally the microwave fluence). Two approaches have already been described in section 6.2 (first image and linear extrapolation from the first two images). A third approach has been tested consisting in fitting the thermogram by a logarithmic polynomial, as in the Thermographic Signal Reconstruction method of references [10, 11]. Figure 8 shows the scatter of the absolute values of the initial adiabatic temperature increase obtained for the three approaches and the frame rates of 1000 Hz, 250 Hz and 125 Hz. Due to the shortness of the plateau, this scatter is probably the main contribution to the uncertainty of the identification. The uncertainty for the two lowest frequency is not acceptable. These results demonstrate the interest to monitor the phenomena with the higher possible frame rate since the uncertainty on the occurrence time of the pulse takes more and more importance when decreasing the frame rate. Furthermore, no strong advantage appears for one of the three approaches tested and a rational choice would need to study several such experiments. Thus, form this study, the optimum choice is taking the simplest approach, which is taking the first image as representative of the first plateau: $\Delta T_{adia} = \Delta T^1$.

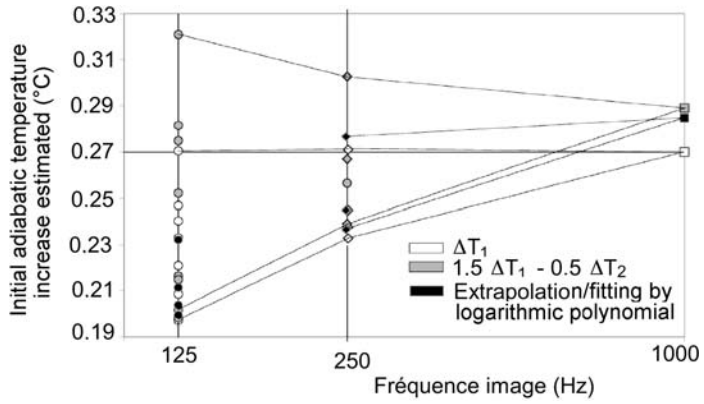

8. *Evaluation of the initial adiabatic plateau level from the thermogram of the ONERA 375 Ω/□ foam-backed film using the three selected approaches*

9. Conclusion

A ruggedized foam-backed screen has been developed at ONERA and tested at the CEA Research Center of Gramat to allow the characterization on the field of very short pulse microwave fields. This type of specialized photothermal screens has been modelled and numerical simulations of their thermal behavior have shown that the identification of the energy deposited by the electromagnetic field is more difficult in this case than using the same sensitive film alone (air-backed film). In particular, the initial adiabatic plateau of the thermograms allowing a simple and sure identification of the fluence is much shorter in the case of the foam-backed film: typically a few milliseconds.

A source of uncertainty lies in the difficulty to obtain a good uniformity of the bonding between the sensitive film and the backing material. Industrializing the fabrication process of the screen could solve this type of problem.

If no synchronization of the microwave pulsed source and the infrared camera exists, both numerical simulations and experiments come to the following conclusions: i) the frame rate of the camera must be equal or higher than 500 images per second, ii), the recommended way to estimate the initial adiabatic temperature increase of the film consists to take the difference of temperature between the first image following the pulse and the last image preceding it.

10. Acknowledgements

This study has been supported by the DGA Research Centre of Gramat (contract DGA n°05 25 049 00 470 46 51).

REFERENCES

[1] Balageas D., Levesque P., Déom A., "Characterization of electromagnetic fields using lock-in IR thermography", Thermosense XV, Proc. SPIE 1933, 1993, pp. 274-285.
[2] Levesque P., Brémond P., Lasserre J.-L., Paupert A., "Performance of FPA IR cameras and of their improvement by time, space and frequency data processing – Part II: Application to the thermographic measurement of microwave fields, QIRT Journal, vol. 2, N° 2, 2005, pp. 237-250.
[3] Norgard J., Sega R., Matini A., Harrison M., "Absorbing screens for IR detection of surface currents", SPIE Proceedings Vol. 780, Thermosense XV, 1993.
[4] Norgard J., Musselman R., "Direct infrared measurement of phased array near-field and far-field antenna patterns", QIRT Journal, vol. 2, N° 1, 2005, pp. 223-236.
[5] Norgard J., Musselman R., "Direct infrared measurement of phased array aperture excitations", QIRT Journal, vol. 2, N° 2, 2005, pp. 113-126.
[6] Maillet D., André S., Batsale J.-C., Degiovanni A., Moyne C., *Thermal quadrupoles – Solving the heat équation through integral transforms*, John Wiley & Sons, Ltd., 2000.
[7] Stehfest H., Numerical inversion of Laplace transforms, Comm. of the ACM, 13,10, 624, 1970.
[8] Balageas D.L., Krapez J.-C., Cielo P., Pulse photothermal modelling of layered materials, J. Appl. Phys., Vol. 59, No 2 (1986), pp. 348-357.
[9] Osiander R., Spicer J.W.M., Time-resolved infrared radiometry with step heating. A review, *Rev .Gen. Therm.,* Vol. 37 (1998), pp. 680-692.
[10] Shepard S.M., Lhota J.R., Rubadeux B.A., Wang D., Ahmed T., "Reconstruction and enhancement of active thermographic image sequences", Optical Engineering, Vol. 42, No 5, May 2003, pp. 1337-1342.
[11] Balageas D.L., Thickness or diffusivity measurements from front-face flash experiments using the TSR (thermographic signal reconstruction) approach*, QIRT 2010 Conference Proc.,* to appear in the Open Archives of QIRT website.